

Article

Revealing Population Connectivity of the Estuarine Tapertail Anchovy *Coilia nasus* in the Changjiang River Estuary and Its Adjacent Waters Using Otolith Microchemistry

Tao Jiang ¹, Hongbo Liu ¹, Yuhai Hu ², Xiubao Chen ¹ and Jian Yang ^{1,2,*} 

¹ Laboratory of Fishery Microchemistry, Freshwater Fisheries Research Center, Chinese Academy of Fishery Sciences, Wuxi 214081, China; jiangt@ffrc.cn (T.J.); liuhb@ffrc.cn (H.L.); chenxb@ffrc.cn (X.C.)

² Wuxi Fisheries College, Nanjing Agricultural University, Wuxi 214081, China; 2020113023@stu.njau.edu.cn

* Correspondence: jianyang@ffrc.cn; Tel./Fax: +86-510-8555-7823

Abstract: The estuarine tapertail anchovy, *Coilia nasus*, is a migratory fish with high economic value in China. We collected fish from the Changjiang River (the Yangtze River) estuary, the Qiantang River estuary, and the southern Yellow Sea, and studied their relationships using otolith elemental and stable isotopic microchemistry signatures to assess the population connectivity of *C. nasus*. Results show that, in addition to Ca, other elements were present in the otolith core. The $\delta^{18}\text{O}$, Na/Ca, Fe/Ca, and Cu/Ca values of the Qiantang population were significantly higher than those of the others, whereas its $\delta^{13}\text{C}$ and Ba/Ca values were found to be significantly lower. Otolith multi-element composition and stable isotope ratios differed significantly between the Qiantang and Changjiang estuary groups ($p < 0.05$); however, no difference was observed between the latter and the Yellow Sea group. Cluster analysis, linear discriminant analysis, and a self-organizing map strongly suggest possible connectivity between the fish populations of the Changjiang estuary and Yellow Sea, while the population of the Qiantang River estuary appears to be independent. Notably, results suggest a much closer connectivity between the fish populations of the Changjiang River and the Yellow Sea.

Keywords: *Coilia nasus*; otolith; river estuary; Yellow Sea; elemental signature; stable isotopic signature



Citation: Jiang, T.; Liu, H.; Hu, Y.; Chen, X.; Yang, J. Revealing Population Connectivity of the Estuarine Tapertail Anchovy *Coilia nasus* in the Changjiang River Estuary and Its Adjacent Waters Using Otolith Microchemistry. *Fishes* **2022**, *7*, 147. <https://doi.org/10.3390/fishes7040147>

Academic Editor: Josipa Ferri

Received: 5 May 2022

Accepted: 22 June 2022

Published: 23 June 2022

Publisher's Note: MDPI stays neutral with regard to jurisdictional claims in published maps and institutional affiliations.



Copyright: © 2022 by the authors. Licensee MDPI, Basel, Switzerland. This article is an open access article distributed under the terms and conditions of the Creative Commons Attribution (CC BY) license (<https://creativecommons.org/licenses/by/4.0/>).

1. Introduction

The connectivity between and identification of different populations of migratory fishes have been the focus of relevant fish surveys and conservation efforts [1–4]. Migration promotes gene exchange among different fish populations and hinders the development of their genetic structuring [5]. In contrast, it builds a bridge for resource flow among different populations. As a result, populations distributed differently in time and space tend to be connected [6,7]. In fact, revealing migration characteristics at a large spatial scale is quite difficult with regard to fishes with a complex habitat history [8,9]. Meanwhile, population connectivity and structure are also difficult to study in this field. Even genetic approaches may not have adequate resolutions, unless straying is negligible over evolutionary time scales [10].

Fortunately, with the development of interdisciplinary fields, otolith, which used to be an important material for the analysis of the age of fish, has increasingly become an important material for studying fish migration ecology. Otoliths, including lapillus, sagitta, and asteriscus, are types of hard tissues located in the fish inner ear, and play an important role in the senses of balance and hearing because of their unique shapes and microcrystalline structures [11]. Although an otolith was originally used as a tool to estimate the age of fish [12,13], analyses of its shape and elemental/isotopic microchemistry have recently demonstrated enormous potential for its use in studies of species, population, or ecosystem-based management [14–19]. Meanwhile, otolith elemental/isotopic chemistry, also termed as otolith microchemistry, is a powerful technique for revealing migration

history, population connectivity of the research object, temporal and spatial distribution characteristics (using elemental signatures) [20–24], dietary changes, and environmental temperature in the species' life-history using stable isotopic signatures [25–28], even with limited (e.g., 2–10) numbers of otolith samples [21,23,29].

The chemical characteristics of otoliths can reflect biographical information of fish habitats throughout their life-history because otoliths are formed before the fish hatches, and elements deposited on them are not metabolized by the fish during their life cycle [30]. In particular, the nucleus region, defined as a small area in the central region of an otolith [31, 32], which usually represents its initial growth period (i.e., larvae and juveniles) [33,34], is important as it corresponds to the fish's incubation and early life-history stage; therefore, the chemical characteristics of the otolith nucleus region can be used to determine the characteristics of hatchery/spawning sites and population origin, which can retrospectively determine the origin of the population [35–37]. In these studies, the elemental "fingerprint" and stable isotope characteristics are often used to determine the physical and chemical nature of the aqueous environment during the incubation and early life-history of research objects for identification and connectivity studies of populations [38,39]. In addition, there are three main channels for element deposition into the otolith: binding with protein in the otolith, inclusion into the calcium carbonate lattice, and substitution of calcium in calcium carbonate crystals [40–42]. The modes of deposition, as observed for the elements, are: (a) Cu and Zn through channel 1, (b) Mg through channel 2, and (c) Sr and Ba through channel 3, which reflect environmental concentrations [42]. The Sr/Ca and Ba/Ca ratios were used as common elemental ratios to study the habitat history and migration patterns of fish because of their direct relationships with the contents of the elements in waterbodies [24,43,44].

The estuarine tapertail anchovy *Coilia nasus* (Temminck et Schlegel, 1846) (junior synonym *Coilia ectenes* (Jordan et Seale, 1905) is a small migratory fish found in large rivers, such as the Changjiang River (the Yangtze River), the Yellow River, and the Qiantang River, and has a high economic value in China. However, its resources are facing a precarious situation because of overfishing and habitat destruction. By contrast, the values of two other ecotype populations, which are *C. nasus taihuensis* (with similar long supermaxilla) and *C. brachygnathus* (with a shorter supermaxilla), are significantly lower, in spite of their relatively substantial resources. As an anadromous fish, the adults migrate from the Yellow Sea and East China Sea upstream along the Changjiang River to spawn in affiliate lakes (e.g., the Poyang Lake), mainly from February to September every year [45]. Notably, the migration patterns of *C. nasus* populations in the Qiantang River are significantly different from those in the Changjiang River [46], indicating that they might be independent populations. In addition, *C. nasus* can be found around the Zhoushan Islands, outside of the mouth of the Qiantang River [47]. The juveniles possibly leave the Changjiang River and move southward into the adjacent East China Sea, and northward into the adjacent Yellow Sea [45]. However, the migration of *C. nasus* from the Qiantang estuary northward to the Yellow Sea has not been reported. Therefore, we hypothesize that *C. nasus* in the Qiantang estuary belong to a resource population with no connectivity to the populations found in the Yellow Sea and the Changjiang River.

The aim of the present study was to assess the population connectivity of *C. nasus* in the Changjiang River and Qiantang River estuaries and the southern Yellow Sea, using an analysis of elemental and stable isotopic microchemistry signatures of the otolith nucleus region of *C. nasus*. The results of the present study could provide a technical basis for the conservation and objective evaluation of *C. nasus* populations in the abovementioned waterbodies.

2. Materials and Methods

2.1. Sampling Sites

The Changjiang river is the main distribution area of *C. nasus*, and the affiliated lakes used to be the spawning grounds. Presently, many lakes along the Changjiang River are blocked by water gates, and only the Dongting Lake, the Poyang Lake, and the Shiju

Lake are believed to be still connected to the river (Figure 1). In our previous work, we confirmed that there was connectivity among *C. nasus* populations in the Poyang Lake, the Changjiang estuary, and the adjacent Yellow Sea [48]. Presently, three waterbodies, including two estuary waters and one sea water, were selected to discover the population connectivity and migration routes of *C. nasus* around the Changjiang estuary (Figure 1). The Jiuduansha Shoal, which used to be a fishing ground of *C. nasus*, is the distributary sandbar located in the southern branch of the Changjiang estuary, with an average depth of 0–6 m. The Qiantang estuary, which is adjacent to the Changjiang estuary, was also selected, to compare the difference in populations with those in the Changjiang River. In addition to these two estuary waters, the coastal waters of the Yellow Sea near Nantong City, which is named the Lvsi fishing ground and is one of the popular fishing grounds in China, was also chosen to detect the possible migration routes of *C. nasus*.

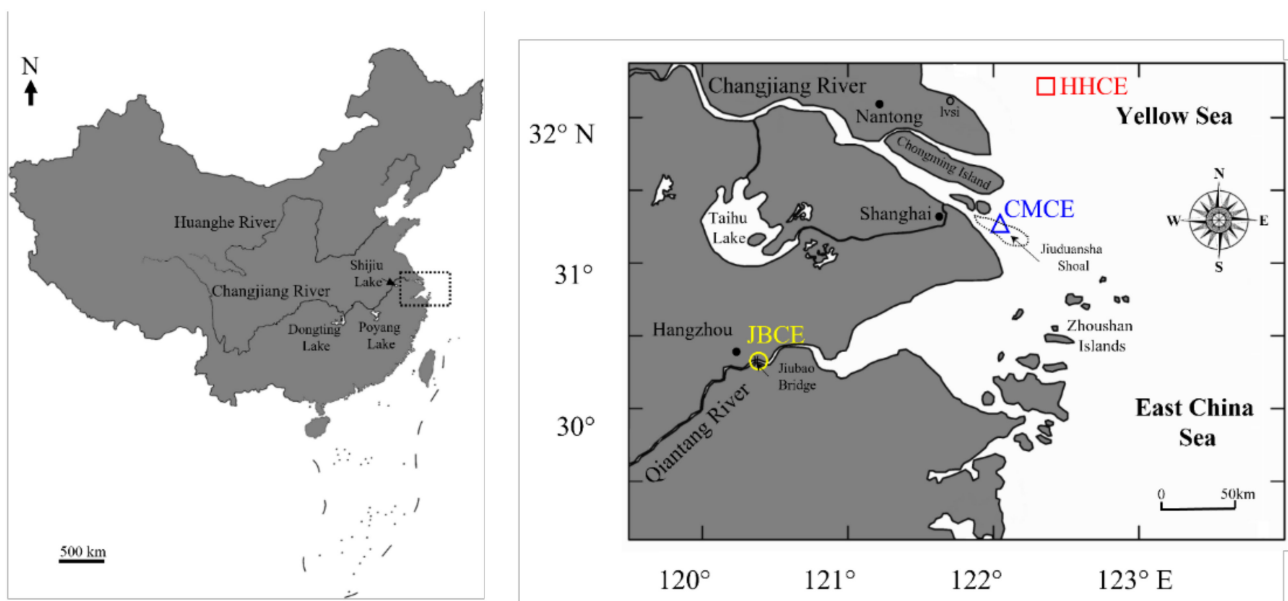


Figure 1. Sampling sites for *Coilia nasus*. Different markers indicate sampling sites in the Nantong coastal area of the Yellow Sea (HHCE, red square), the Changjiang estuary near the Jiuduansha Shoal (CMCE, blue triangle), and the Jiubao bridge waters in the Qiantang estuary (JBCE, yellow circle), from north to south.

2.2. Experimental Fish

Thirty *C. nasus* specimens were collected from the Qiantang estuary near the Jiubao Bridge waters (JBCE, 120.3° E, 30.3° N) in April 2016, the Changjiang estuary near the Jiuduansha Shoal (CMCE, 122.1° E, 31.2° N) in April 2016, and the coastal waters of the Yellow Sea near Nantong City (HHCE, 122.2° E, 32.2° N) in May 2016 (Figure 1). Sagittal otoliths were extracted from these specimens after measuring their total length and body weight (Table 1). After cleaning, the otoliths were embedded in epoxy resin (Epofix; Struers, Copenhagen, Denmark) with the proximal surface upside. The otoliths were then ground by a grinding machine (Discoplan-TS, Struers, Copenhagen, Denmark) to expose the cores and polished using an automated polishing machine (Roto Pol-35; Struers, Copenhagen, Denmark) with a polishing solution (OP-S NonDry, Struers, Copenhagen, Denmark) to remove scratches on the surface. Following this, a flat surface through the core of each otolith was obtained. After checking the annulus and determining the age of each otolith, the samples were cleaned in an ultrasonic bath, rinsed with Milli-Q water (Millipore, Molsheim, France), and oven-dried at 38 °C overnight.

Table 1. Sampling details of *Coilia nasus* in the present study.

Sampling Site	Sample Code	Sampling Date	Sample Size (N)	Total Length (mm)	Body Weight (g)	Age ^a (Year)	Gonad Stage ^b
Coastal water in the Yellow Sea near Nantong City	HHCE	13 April 2016	10	261 ± 14	49.00 ± 15.56	2	II
Changjiang River estuary near Jiuduansha Shoal	CMCE	1–5 April 2016	10	284 ± 10	64.61 ± 7.75	2	II (2 ind.) III (8 ind.)
Qiantang River estuary near Jiubao bridge waters	JBCE	10 May 2016	10	271 ± 12	46.85 ± 7.79	2	III

Note: ^a Fish age was determined by the annuli in the otolith [49]. ^b Gonad stages of maturation were determined by visual examination of the gonads [50,51], i.e., stage II (developmental stage), stage III (early mature stage), etc.

2.3. Elemental Analysis

Elemental signature analysis of the otolith nucleus region, which was estimated at 0–1 month [52], was performed at the Laboratory of Fishery Microchemistry at the Freshwater Fisheries Research Center, Wuxi, China, using an NW213 laser ablation system (New Wave Research, Fremont, CA, USA) coupled with an Agilent 7500ce ICPMS (Agilent Technologies, Wilmington, DE, USA). Nineteen elements, including Li, Na, Mg, Al, K, Ca, Sc, Ti, V, Cr, Mn, Fe, Co, Ni, Cu, Zn, Sr, Cd, and Ba, were analyzed with a laser wavelength of 213 nm. The applied voltage, pulse rate, energy intensity, and residence time were 10 kV, 10 Hz, 11.76 J/cm², and 5 s, respectively. Because the nucleus region was defined as the round area that spreads at a radius of 190–230 µm from the core [53], a smaller beam width of 80 µm, which was estimated at approximately 10 d based on our unpublished work and previous literature [52], was selected for ablating the nucleus regions of all samples.

NIST612 and MACS-3 were used as the standards and analyzed after every 10 samples; 100-s blank data were used as the background signal to calculate the limits of detection (LOD) before and after the analysis. All results were expressed as the molecular weight ratio (mmol/mol) of the element to Ca. During the analysis, the relative standard deviation (RSD) of the corresponding elemental ratio in the signal of the standard sample was calculated to determine the signal stability (RSD% < 10).

2.4. Stable Isotope Analysis

Stable isotope analysis was also performed at the Laboratory of Fishery Microchemistry, Freshwater Fisheries Research Center, Wuxi, China. After elemental analysis, the otoliths were repolished to remove the laser ablation burn scars and cleaned in an ultrasonic bath, rinsed with Milli-Q water (Millipore, Molsheim, France), and oven-dried at 38 °C overnight. A MicroMill (New Wave Research, Fremont, CA, USA) micro-sampler was used to drill the nucleus region (see Figure 2), and powdered samples were collected. For adequate signals, the depth was set as 300 µm, while the diameter of the drilling hole was 198.1 ± 2.5 µm in the central parts of the aforementioned otolith core areas [53], which were estimated at approximately 25 d based on our unpublished data and a previous report [52]. Otolith isotope analysis was performed using a Delta V Advantage stable isotope ratio mass spectrometer equipped with a Gas Bench II Gas generator (Thermo Fisher Scientific, Waltham, MA, USA). The samples were placed at the bottom of glass test tubes (QSA00303, Thermo Fisher Scientific) before analysis. The natural abundance of carbon/oxygen stable isotope was expressed as follows:

$$\delta X (\text{‰}) = [(R_{\text{otolith}} - R_{\text{standard}}) / R_{\text{standard}}] \times 1000$$

where X represents $\delta^{13}\text{C}$ and $\delta^{18}\text{O}$ and R represents the $^{13}\text{C}/^{12}\text{C}$ or $^{18}\text{O}/^{16}\text{O}$ ratio. The accuracies of $\delta^{13}\text{C}$ and $\delta^{18}\text{O}$ detection were monitored against an isotope standard (NBS 18, International Atomic Energy Agency, Vienna, Austria) and expressed using Vienna Pee Dee Belemnite (VPDB) as an international standard unit. The precision of the analyses based on the measurements of this standard was within 0.03%.

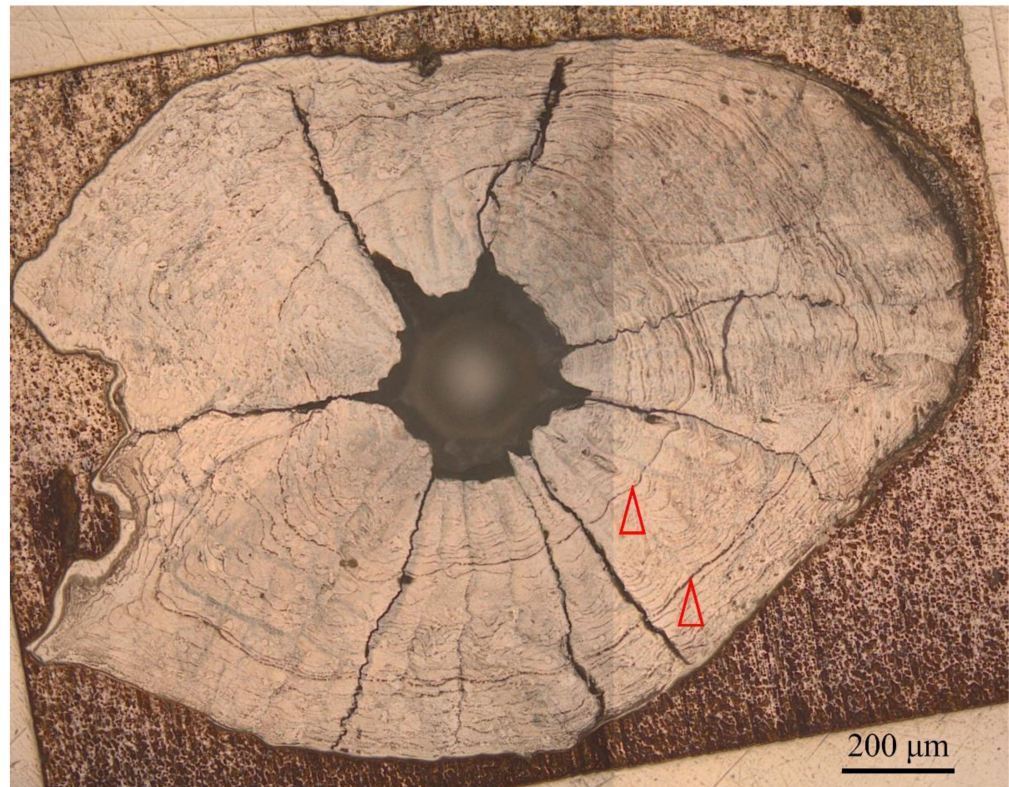


Figure 2. Otolith after drilling of the nucleus region. The red triangles show the annuli.

2.5. Statistical Analysis

The homogeneity of variance and the normality of the distribution of all data were checked using SPSS 23.0 (IBM SPSS Statistics Inc., Chicago, IL, USA). Multiple analysis of variance (MANOVA) and one-way analysis of variance (ANOVA) were carried out to assess the differences among all three groups and between independent groups using SPSS 23.0 (IBM SPSS Statistics Inc.). All elemental and stable isotopic ratios were centered using the Z-Score and displayed using the pheatmap (v 1.0.12) package in R (Ver. 4.1.2). A cluster analysis was also performed based on the complete linkage method, with Euclidean distance as the distance measuring method using the same package. The ratios were further examined using principal component analysis (PCA) and linear discriminant analysis (LDA) in SPSS 23.0 and self-organizing map (SOM) analysis, with the help of the Toolbox2.0 toolkit in Matlab 9.0 (Mathworks, Inc., El Segundo, CA, USA), to study the relationships between the groups. The map size was set according to $5 \times (\text{number of samples})^{\frac{1}{2}}$ [54], and then based on the minimizing quantization error (QE) and topographic error (TE) [55]. The number of groups was set mainly based on the clustering analysis. The cells were then divided into different groups according to the similarity of the weight vectors of the neurons by Ward's linkage method [56].

3. Results

3.1. Elemental Ratios in the Otolith Nucleus Regions of *C. nasus*

In addition to Ca, we detected Na, Mn, Fe, Ni, Cu, Sr, and Ba in the samples with %RSD ranging from 2.05 (Sr/Ca) to 8.5 (Ni/Ca), and LODs (mmol/mol) for Na/Ca (0.031), Mn/Ca (6.2×10^{-4}), Fe/Ca (0.0051), Ni/Ca (6.4×10^{-5}), Cu/Ca (1.1×10^{-4}), Sr/Ca (6.6×10^{-4}), and Ba/Ca (3.2×10^{-6}), based on the standards (Table 2). Apart from Mn/Ca and Sr/Ca, for which there were no significant differences among the three groups, there was no significant difference between the specimens of HHCE and CMCE in the elemental ratios ($p > 0.05$). Meanwhile, four elemental ratios determined in the present study- Na/Ca,

Fe/Ca, Ni/Ca, and Ba/Ca- were significantly different between the specimens of CMCE and JBCE ($p < 0.05$) (Table 2).

Table 2. Elemental ratios in the otolith nucleus regions of *Coilia nasus*.

Item	Elemental Ratio (mmol/mol)						
	Na/Ca	Mn/Ca	Fe/Ca	Ni/Ca	Cu/Ca	Sr/Ca	Ba/Ca
RSD (%)	7.33	5.42	2.31	8.50	6.25	2.05	3.14
LOD	0.031	6.20×10^{-4}	0.0051	6.40×10^{-5}	1.10×10^{-4}	6.60×10^{-6}	3.20×10^{-6}
HHCE	8.73 ± 0.3^a	0.012 ± 0.008^a	0.43 ± 0.01^a	0.0077 ± 0.0011^{ab}	0.00030 ± 0.00007^a	0.69 ± 0.14^a	0.013 ± 0.006^{ab}
CMCE	8.51 ± 0.36^a	0.011 ± 0.01^a	0.42 ± 0.01^a	0.0072 ± 0.0007^b	0.00035 ± 0.00015^{ab}	0.70 ± 0.10^a	0.017 ± 0.005^b
JBCE	9.15 ± 0.3^b	0.005 ± 0.005^a	0.46 ± 0.01^b	0.0082 ± 0.0009^a	0.00043 ± 0.00008^b	0.74 ± 0.21^a	0.009 ± 0.004^a

Note: Different superscript letters in each column indicate significant differences between groups ($p < 0.05$). *C. nasus* collected in the Nantong coastal region of the Yellow Sea (HHCE), *C. nasus* collected in the Changjiang estuary near the Jiuduansha Shoal (CMCE), and *C. nasus* collected in the Jiubao Bridge waters in the Qiantang estuary (JBCE). Data are mean \pm standard deviation.

3.2. Stable Isotopic Ratios in the Otolith Nucleus Regions of *C. nasus*

The $\delta^{13}\text{C}$ and $\delta^{18}\text{O}$ in the otolith nucleus region of *C. nasus* showed no significant differences between HHCE and CMCE ($p > 0.05$). The $\delta^{13}\text{C}$ of JBCE was lower than that of the other groups, while $\delta^{18}\text{O}$ was higher to a very significant extent ($p < 0.05$) (Table 3).

Table 3. Stable isotopic ratios in the otolith nucleus regions of *Coilia nasus*.

Group	Stable Isotopic Ratios (‰, VPDB)	
	$\delta^{13}\text{C}$	$\delta^{18}\text{O}$
HHCE	-10.42 ± 1.81^a	-7.72 ± 1.79^a
CMCE	-10.31 ± 1.49^a	-7.32 ± 0.93^a
JBCE	-13.12 ± 1.00^b	-4.08 ± 0.72^b

Note: Different superscript letters in each column indicate significant differences ($p < 0.05$). *C. nasus* collected in the Nantong coastal region of the Yellow Sea (HHCE), *C. nasus* collected in the Changjiang estuary near the Jiuduansha Shoal (CMCE), and *C. nasus* collected in the Jiubao Bridge waters in the Qiantang estuary (JBCE). Data are mean \pm standard error.

3.3. Multivariate Statistics Based on Elemental and Stable Isotopic Ratios

Results of the MANOVA indicated that there was no significant difference between the HHCE and CMCE specimens ($p > 0.05$). However, significant differences were observed between JBCE and the other specimens ($p < 0.05$).

The $\delta^{18}\text{O}$, Na/Ca, Fe/Ca, and Cu/Ca values of *C. nasus* in JBCE were found to be higher (red boxes) than those in the other populations, while $\delta^{13}\text{C}$ and Ba/Ca values were found to be lower (blue box) (Figure 3). According to these elemental and stable isotope ratios, the results of the cluster analysis showed that the *C. nasus* of JBCE formed a distinct single group, while the individuals of HHCE and CMCE showed a mixed pattern. Consistent with this result, PCA also clearly showed that the individuals of HHCE and CMCE were mixed well, while those of JBCE were independent from the others (Figure 4).

Cross-validation through LDA showed that the discriminant accuracy of *C. nasus* of HHCE and CMCE was 60%. The remaining 40% were misjudged as individuals of each other's groups. The discriminant accuracy for the JBCE group was 100%, which was different from that of the other two groups (Table 4 and Figure 5).

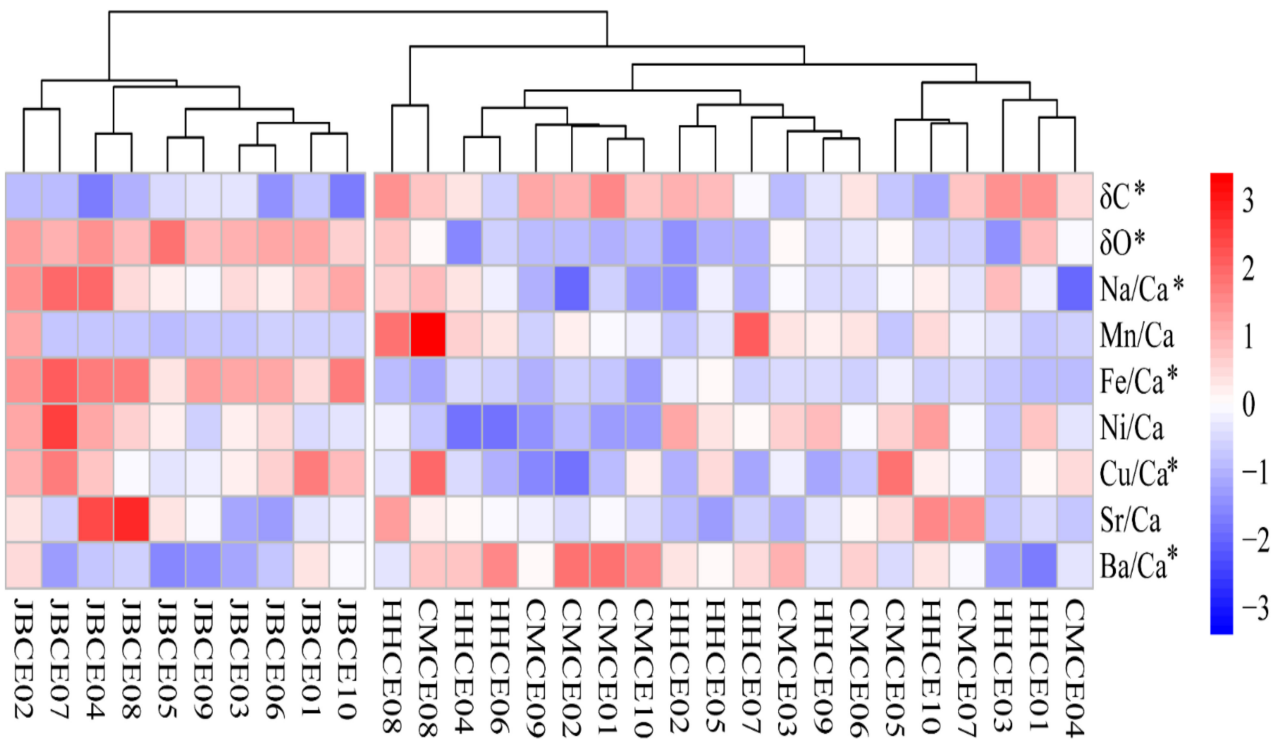


Figure 3. Microchemical characteristics of *Coilia nasus* from the Nantong coastal area of the Yellow Sea (HHCE), the Changjiang estuary near the Jiuduansha Shoal (CMCE), and the Jiubao bridge waters in the Qiantang estuary (JBCE), based on the Pheatmap. The different shades of blue and red reflect different values. The (*) symbol represents a significant difference ($p < 0.05$, one-way ANOVA).

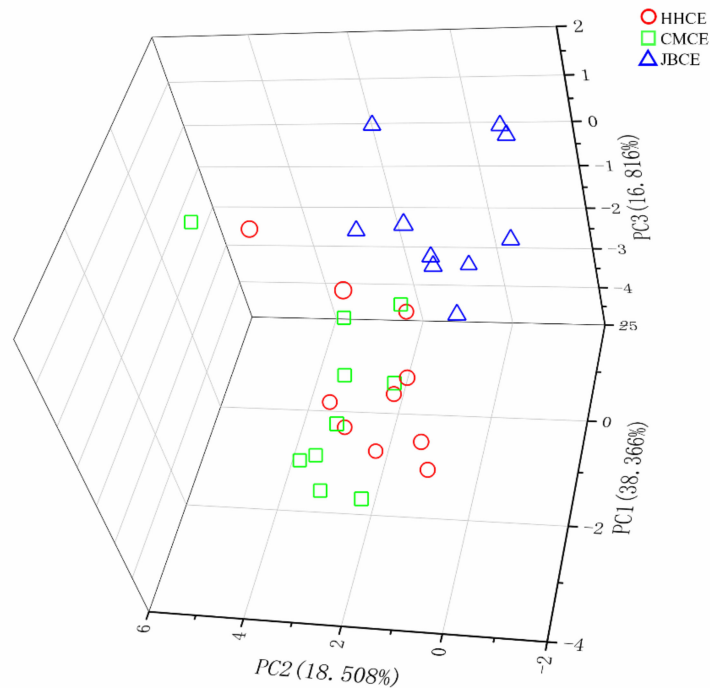


Figure 4. Principal component analysis of *Coilia nasus* from the Nantong coastal area of the Yellow Sea (HHCE), the Changjiang estuary near the Jiuduansha Shoal (CMCE), and the Jiubao bridge waters in the Qiantang estuary (JBCE), based on microchemical characteristics of the otolith core. Those of HHCE and CMCE were mixed well, while those of JBCE were independent from the others.

Table 4. Linear discriminant analysis of *Coilia nasus* populations in the Yellow Sea (HHCE), the Changjiang estuary (CMCE), and the Qiantang estuary (JBCE) based on $\delta^{13}\text{C}$, $\delta^{18}\text{O}$, and elemental ratio characteristics in the otolith nucleus region.

	Group	Predicted Group (Original/Cross-Validated)		
		HHCE	CMCE	JBCE
Count	HHCE	6 (6)	4 (4)	0 (0)
	CMCE	3 (4)	7 (6)	0 (0)
	JBCE	0 (0)	0 (0)	10 (10)
%	HHCE	60 (60)	40 (40)	0 (0)
	CMCE	30 (40)	70 (60)	0 (0)
	JBCE	0 (0)	0 (0)	100 (100)

Note: HHCE: *C. nasus* collected in the Nantong coastal region of the Yellow Sea. CMCE: *C. nasus* collected in the Changjiang estuary near the Jiuduansha Shoal. JBCE: *C. nasus* collected in the Jiubao Bridge waters in the Qiantang estuary.

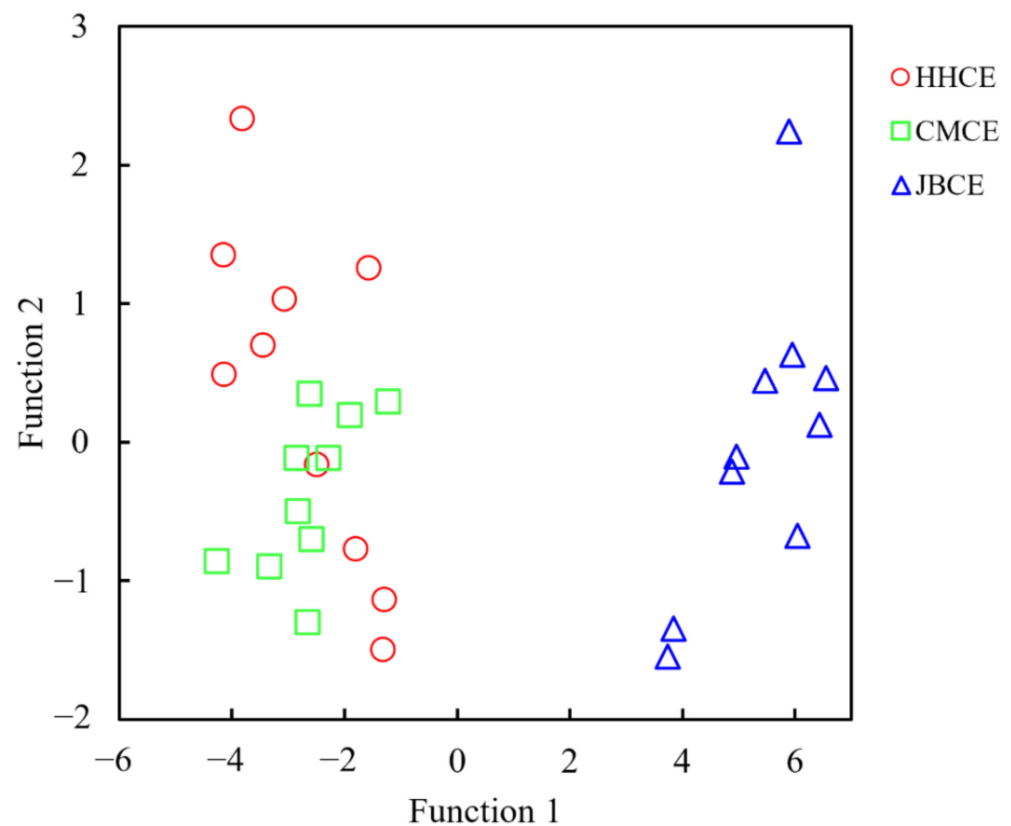


Figure 5. Discriminant analysis of *Coilia nasus* from the Nantong coastal area of the Yellow Sea (HHCE), the Changjiang estuary near the Jiuduansha Shoal (CMCE), and the Jiubao bridge waters in the Qiantang estuary (JBCE), based on microchemical characteristics of the otolith core. Those of HHCE and CMCE were mixed, while those of JBCE were independent from the others.

The SOM analysis also clearly indicated a similar relationship. Results showed that the JBCE was clearly distinguished from the other two populations (CMCE and HHCE). The latter two populations gathered into a large group with 25 (5×5) output cells, corresponding to 30 samples from three waterbodies, which could obtain the best network training effect with QE and TE values of 0.345 and 0.024, respectively (Figure 6).

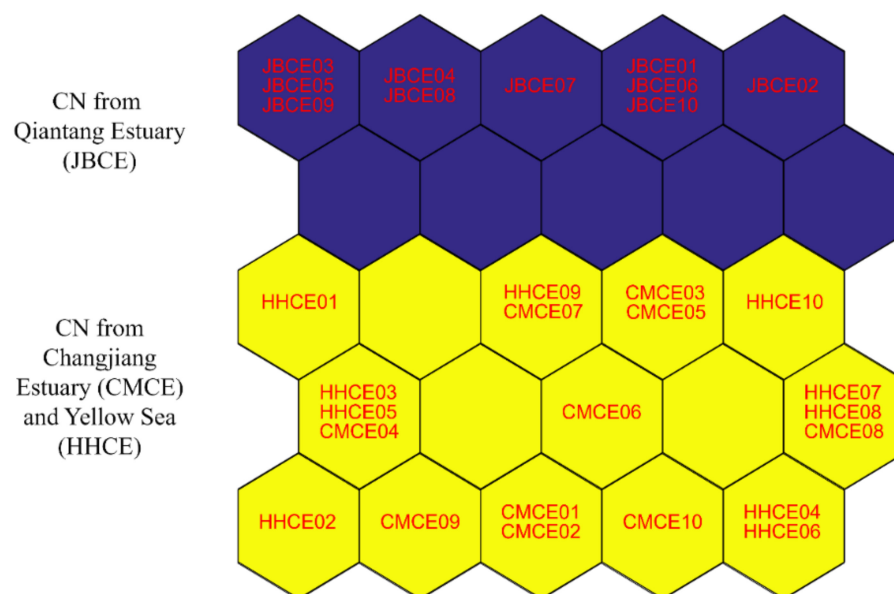


Figure 6. Self-organizing map (SOM) analysis of *Coilia nasus* from the Nantong coastal area of the Yellow Sea (HHCE), the Changjiang estuary near the Jiuduansha Shoal (CMCE), and the Jiubao bridge waters in the Qiantang estuary (JBCE). Those of HHCE and CMCE were mixed in yellow cells, while those of JBCE were independent of the others in blue cells.

4. Discussion

The deposition mechanisms of different elements were distinct and were derived from ambient waterbodies. Consequently, the interannual changes in otolith elements were smaller than their spatial differences [57–59]. Therefore, in addition to Sr/Ca and Ba/Ca ratios, the ratios of other elements to Ca in special areas of otoliths (such as core areas corresponding to hatcheries) may also reflect the differences in the research objects, and these may be used to understand population structures and connectivity characteristics [37,58]. The elemental ratios Na/Ca, Mn/Ca, Fe/Ca, Ni/Ca, Cu/Ca, Sr/Ca, and Ba/Ca were selected according to a previous study [48], and the present results suggested that those elemental characteristics could be used as natural tags in discriminating *C. nasus* of the Changjiang Estuary and adjacent waterbodies.

The stable isotopic ratios were significantly different between the *C. nasus* from the Qiantang estuary and those from the Changjiang estuary and the Yellow Sea. Notably, juveniles of *C. nasus* usually live in freshwater during their first year of growth [60]. The length the otolith of *C. nasus* during its early life history in the freshwater was $980 \pm 111 \mu\text{m}$ [47], which means that the materials extracted from a hole with a diameter of $200 \mu\text{m}$ (corresponding to an age of 25 d) in the nucleus region mainly reflect the early freshwater life-history in their natal river. Therefore, the respective region should also be named as the “natal region.” In addition to regional differences, the differences in $\delta^{18}\text{O}$ between otoliths and water was negatively correlated with water temperature, and therefore it can be used as an indicator of ambient water temperature [25,61]. The significant differences between the populations of *C. nasus* in the Qiantang estuary and those in the Yellow Sea and the Changjiang estuary may mainly reflect the differences in the average water temperatures during the early life of *C. nasus*. The higher $\delta^{18}\text{O}$ of *C. nasus* in the Qiantang estuary, the lower the temperature of this waterbody compared to that of the Changjiang River and the Yellow Sea. This may result in earlier breeding of *C. nasus* in the Qiantang River. The Qiantang River is located south of the Changjiang River. These facts are consistent with the report that the populations of *C. nasus* in the northern waterbodies start migration in May–June, while the populations in the southern region, such as the Changjiang estuary, start in March [62]. Future studies can advantageously use our results for the determination of exact spawning times and locations. Furthermore, future studies should consider more

diverse environments, in order to reveal the relationship between chemical information obtained from otoliths and environmental conditions.

Both water temperature and $\delta^{13}\text{C}$ in ambient water can partly influence the content of $\delta^{13}\text{C}$ in the otolith [63,64]; however, the diet condition of the fish will continue to have the most important role [65,66]. Results indicated that the populations of *C. nasus* in the Yellow Sea and the Changjiang estuary were significantly greater than that in the Qiantang estuary. Previous studies have shown that the Poyang Lake is one of the important spawning grounds for the migratory population in the Changjiang River, while there is no large lake to serve as a spawning ground along the Qiantang River. Therefore, the food conditions that *C. nasus* experiences during its early life are expected to be different between the Yellow Sea and Changjiang estuary, that have a higher $\delta^{13}\text{C}$, and the Qiantang estuary, that has a lower $\delta^{13}\text{C}$.

In the present study, the gonad development of most *C. nasus* fish of both the Changjiang and Qiantang populations were at gonad stage III (Table 2), indicating that both populations were reproductive [50] and that their spawning sites were located in the corresponding rivers, as they had already migrated into the estuary waters. As previously mentioned, the analyzed nucleus region represented approximately 10-d and 25-d life histories in the larva stage [52]. Although there was no report on how fast the larvae can move or drift from their originating locations (i.e., spawning site and hatchery) until now, results of both the trace elemental and isotopic ratios reflect the conditions prevailing in their originating rivers during such a short period, and in addition, during their first year of growth in freshwater [60]. Results of multivariate statistics, based on the elemental and stable isotopic ratios, clearly reveal the possibility of connectivity among the populations of the three waterbodies. Although the sample size was relatively low in the present study, the cluster analysis, PCA, LDA, and SOM clearly show that *C. nasus* in the Qiantang estuary is a population that is independent of those in the Changjiang and the Yellow Sea, which is consistent with previous studies that have revealed significant differences in the life history of the Qiantang population with those of the Changjiang and the Yellow Sea [46,47,60]. Meanwhile, the population of the Yellow Sea mixed well with that of the Changjiang, indicating the possibility of connectivity between these two populations. In addition, the Qiantang and Changjiang Rivers are adjacent to each other. Findings of previous [46,47] and the present study indicated that some individuals can be “mixed” or “lost” in the two adjacent rivers during the migratory season, which strongly suggests that the adults can recognize and return to their natal river for spawning, which highlights a strong “natal homing” feature in the species, like in the case of salmon [67].

Results of the present study clearly indicate the connectivity between the fish populations in the Changjiang estuary and the Yellow Sea. This is in accordance with the results of our previous study, in which samples were gathered in 2011–2012 [48]. Therefore, the results of both these studies suggest that some juveniles from the Changjiang River swam northeast into the Yellow Sea after almost one year of freshwater life history [60]. By contrast, there was no connectivity between the JBCE and HHCE populations, which were randomly sampled during the migratory season, as suggested by their different life histories and migratory patterns [46,60]. Because of the low sample size, the ability of the Qiantang population to move north into the Yellow Sea could not be confirmed; however, the results imply a stronger connectivity between the Yellow Sea and Changjiang populations than with the Qiantang population.

Knowledge on the fine scale natal origin of the anadromous fish *C. nasus* is difficult to obtain because of gaps in knowledge on their distribution in spawning sites and in surveys of resources during their early growth stage. Fortunately, we discovered a spawning site in the Poyang Lake, the largest freshwater lake in China, which is affiliated to the Changjiang River [68]. We expect that other spawning sites are likely to exist along the river [48]. The elemental ratios or $\delta^{13}\text{C}$ and $\delta^{18}\text{O}$ in the otoliths provide adequate information on the connectivity among different populations, compared with establishing connectivity based on the identification of original locations (i.e., spawning/hatchery site) without considering a special population, such as fully mature adults within the spawning site [48] or weakly

swimming larvae and juveniles within the natal waters [10]. However, the strontium isotope ratio ($^{87}\text{Sr}/^{86}\text{Sr}$) in the otolith seems to accurately delineate the natal origin at a fine scale, as it has a high correlation with that of ambient waters with spatial features at a fine scale [69]. In the future, a robust framework should be built based on the strontium isotope ratios of both the otoliths and habitat waters of *C. nasus*, which will play an important role in assessing natal sources at a fine spatial scale and delineate its detailed migratory route during different developmental stages.

In addition, the results of this study show that the *C. nasus* population in the Yellow Sea enters the Qiantang estuary, and that from the Qiantang estuary it enters into the Yellow Sea or the Changjiang River estuary. This indicates that *C. nasus* migration may be very accurate, like that of salmon migration. Salmon primarily relies on smell to locate hatching/spawning sites accurately [70]. A similar olfactory gene was also found in *C. nasus* [71]. Therefore, *C. nasus* may also use “olfactory” memories to return to their hatcheries for breeding. This behavior of migratory fish, in which a population can return to respective spawning ground with a high success rate of hatching, is known as natal homing, and it guarantees a considerable population reproduction success rate [5]. It is likely that *C. nasus* displays similar behavior.

5. Conclusions

The aforementioned results of otolith microchemistry strongly suggest that there are two natal original populations in the Qiantang and Changjiang Rivers. They also suggest that the population in the Yellow Sea has little connectivity with that of the Qiantang River, but that it had a supplementary relationship with that of the Changjiang River. Nevertheless, whether the population of the Qiantang can move north into the Yellow Sea remains to be confirmed because of the limitation of the low sample size of the present study and the knowledge gaps on the marine life histories and fine scale natal origins of these three populations. Consequently, future research should focus on the connectivity of populations of *C. nasus*, which inhabit the South–East China Sea and the adjacent river estuaries, based on otolith microchemistry and assessment of environmental conditions (i.e., water temperature, salinity, etc.), to determine the migratory dynamics of the Changjiang, Qiantang, and other southern populations. Furthermore, the elemental characteristics of the otolith from the core to the edge, and a robust framework based on strontium isotope ratios of both otolith and waters, must be studied to arrive at a more accurate migration route, in order to assess the finer-scale natal origin of *C. nasus*. In addition, as there is the possibility of natal homing behavior, resource estimation and conservation work should be carried out for different populations of *C. nasus*.

Author Contributions: Conceptualization, T.J., J.Y., H.L., and X.C.; Methodology, T.J., H.L., Y.H., X.C., and J.Y.; Investigation, T.J., H.L., Y.H., and J.Y.; Resources, T.J. and J.Y.; Funding acquisition, T.J. and J.Y.; Writing—Original Draft, T.J., H.L., Y.H., and X.C.; Writing—Review & Editing, J.Y.; Supervision, J.Y. All authors have read and agreed to the published version of the manuscript.

Funding: This research was funded by the Central Public-interest Scientific Institution Basal Research Fund, Freshwater Fisheries Research Center, CAFS (2021JBFM14), and the Central Public-interest Scientific Institution Basal Research Fund, CAFS (2021GH08).

Institutional Review Board Statement: The study was conducted according to the guidelines of the Declaration of Helsinki. All *Coilia nasus* samples were dead individuals from legal commercial fisheries. Therefore, there was no need to apply for an approval by the Animal Ethics Committee.

Informed Consent Statement: Not applicable.

Data Availability Statement: The data that support the findings of this study are available from the corresponding author upon reasonable request.

Conflicts of Interest: The authors declare no conflict of interest.

References

1. Avigliano, E.; Carvalho, B.; Velasco, G.; Tripodi, P.; Vianna, M.; Volpedo, A.V. Nursery areas and connectivity of the adult anadromous catfish (*Genidens barbatus*) revealed by otolith-core microchemistry in the south-western Atlantic Ocean. *Mar. Freshw. Res.* **2017**, *68*, 931–940. [[CrossRef](#)]
2. Rohtla, M.; Matetski, L.; Svirgsden, R.; Kesler, M.; Taal, I.; Saura, A.; Vaittinen, M.; Vetemaa, M. Do sea trout *Salmo trutta* parr surveys monitor the densities of anadromous or resident maternal origin parr, or both? *Fish. Manag. Ecol.* **2017**, *24*, 156–162. [[CrossRef](#)]
3. Koeberle, A.L.; Arismendi, I.; Crittenden, W.; Di Prinzio, C.; Gomez-Uchida, D.; Noakes, D.L.G.; Richardson, S. Otolith shape as a classification tool for Chinook salmon (*Oncorhynchus tshawytscha*) discrimination in native and introduced systems. *Can. J. Fish. Aquat. Sci.* **2020**, *77*, 1172–1188. [[CrossRef](#)]
4. Beacham, T.D.; Wallace, C.G.; Jonsen, K.; McIntosh, B.; Candy, J.R.; Horst, K.; Lynch, C.; Willis, D.; Luedke, W.; Kearey, L.; et al. Parentage-based tagging combined with genetic stock identification is a cost-effective and viable replacement for coded-wire tagging in large-scale assessments of marine Chinook salmon fisheries in British Columbia, Canada. *Evol. Appl.* **2021**, *14*, 1365–1389. [[CrossRef](#)] [[PubMed](#)]
5. McDowall, R.M. Diadromy, diversity and divergence: Implications for speciation processes in fishes. *Fish Fish.* **2001**, *2*, 278–285. [[CrossRef](#)]
6. Torniaainen, J.; Vuorinen, P.J.; Jones, R.I.; Keinänen, M.; Palm, S.; Vuori, K.A.M.; Kiljunen, M. Migratory connectivity of two Baltic Sea salmon populations: Retrospective analysis using stable isotopes of scales. *ICES J. Mar. Sci.* **2014**, *71*, 336–344. [[CrossRef](#)]
7. Alshwairikh, Y.A.; Kroeze, S.L.; Olsson, J.; Stephens-Cardenas, S.A.; Swain, W.L.; Waits, L.P.; Horn, R.L.; Narum, S.R.; Seaborn, T. Influence of environmental conditions at spawning sites and migration routes on adaptive variation and population connectivity in Chinook salmon. *Ecol. Evol.* **2021**, *11*, 16890–16908. [[CrossRef](#)]
8. Arai, T. Migration ecology in the freshwater eels of the genus *Anguilla* Schrank, 1798. *Trop. Ecol.* **2022**, *6*, e05176. [[CrossRef](#)]
9. Miller, M.J.; Yoshinaga, T.; Aoyama, J.; Otake, T.; Mochioka, N.; Kurogi, H.; Tsukamoto, K. Offshore spawning of *Conger myriaster* in the western North Pacific: Evidence for convergent migration strategies of anguilliform eels in the Atlantic and Pacific. *Naturwissenschaften* **2011**, *98*, 537–543. [[CrossRef](#)]
10. Thorrold, S.R.; Latkoczy, C.; Swart, P.K.; Jones, C.M. Natal homing in a marine fish metapopulation. *Science* **2001**, *291*, 297–299. [[CrossRef](#)]
11. Schulz Mirbach, T.; Ladich, F.; Plath, M.; Heß, M. Enigmatic ear stones: What we know about the functional role and evolution of fish otoliths. *Biol. Rev.* **2019**, *94*, 457–482. [[CrossRef](#)] [[PubMed](#)]
12. Burton, M.L.; Potts, J.C.; Ostrowski, A.D.; Shertzer, K.W. Age, growth, and natural mortality of Graysby, *Cephalophilis cruentata*, from the southeastern United States. *Fishes* **2019**, *4*, 36. [[CrossRef](#)]
13. Burton, M.L.; Potts, J.C.; Ostrowski, A.D. Preliminary estimates of age, growth and natural mortality of margate, *Haemulon album*, and black margate, *Anisotremus surinamensis*, from the Southeastern United States. *Fishes* **2019**, *4*, 44. [[CrossRef](#)]
14. Geffen, A.J.; Morales-Nin, B.; Gillanders, B.M. Fish otoliths as indicators in ecosystem based management: Results of the 5th International Otolith Symposium (IOS2014). *Mar. Freshw. Res.* **2016**, *67*, i–iv. [[CrossRef](#)]
15. D'Iglio, C.; Albano, M.; Famulari, S.; Savoca, S.; Panarello, G.; Di Paola, D.; Perdichizzi, A.; Rinelli, P.; Lanteri, G.; Spano, N.; et al. Intra- and interspecific variability among congeneric *Pagellus* otoliths. *Sci. Rep.* **2021**, *11*, 16315. [[CrossRef](#)]
16. D'Iglio, C.; Natale, S.; Albano, M.; Savoca, S.; Famulari, S.; Gervasi, C.; Lanteri, G.; Panarello, G.; Spanò, N.; Capillo, G. Otolith analyses highlight morpho-functional differences of three species of mullet (Mugilidae) from transitional water. *Sustainability* **2022**, *14*, 398. [[CrossRef](#)]
17. Mitsui, S.; Strüßmann, C.A.; Yokota, M.; Yamamoto, Y. Comparative otolith morphology and species identification of clupeids from Japan. *Ichthyol. Res.* **2020**, *67*, 502–513. [[CrossRef](#)]
18. D'Iglio, C.; Albano, M.; Tiralongo, F.; Famulari, S.; Rinelli, P.; Savoca, S.; Spanò, N.; Capillo, G. Biological and ecological aspects of the blackmouth catshark (*Galeus melastomus* Rafinesque, 1810) in the Southern Tyrrhenian Sea. *J. Mar. Sci. Eng.* **2021**, *9*, 967. [[CrossRef](#)]
19. Polito, M.J.; Trivelpiece, W.Z.; Karnovsky, N.J.; Ng, E.; Patterson, W.P.; Emslie, S.D. Integrating stomach content and stable isotope analyses to quantify the diets of pygoscelid penguins. *PLoS ONE* **2011**, *6*, e26642. [[CrossRef](#)]
20. Chino, N.; Arai, T. Migratory history of the fourspine sculpin *Rheopresbe kazika*, a national monument species in Japan. *Thalassa* **2020**, *36*, 395–398. [[CrossRef](#)]
21. Tran, N.T.; Labonne, M.; Chung, M.T.; Wang, C.H.; Huang, K.F.; Durand, J.D.; Grudpan, C.; Chan, B.; Hoang, H.D.; Panfili, J. Natal origin and migration pathways of Mekong catfish (*Pangasius krempfi*) using strontium isotopes and trace element concentrations in environmental water and otoliths. *PLoS ONE* **2021**, *16*, e0252769. [[CrossRef](#)] [[PubMed](#)]
22. Rohtla, M.; Matetski, L.; Taal, I.; Svirgsden, R.; Kesler, M.; Paiste, P.; Vetemaa, M. Quantifying an overlooked aspect of partial migration using otolith microchemistry. *J. Fish Biol.* **2020**, *97*, 1582–1585. [[CrossRef](#)] [[PubMed](#)]
23. Avigliano, E.; Pisonero, J.; Mendez, A.; Tombari, A.; Volpedo, A.V. Habitat use of the amphidromous catfish *Genidens barbatus*: First insights at its southern distribution limit. *N. Z. J. Mar. Fresh.* **2021**, *263*, 107637. [[CrossRef](#)]
24. Xiong, Y.; Yang, J.; Jiang, T.; Liu, H.B.; Zhong, X.M.; Xiong, Y.; Yang, J.; Jiang, T.; Liu, H.; Zhong, X.; et al. Temporal stability in the otolith Sr:Ca ratio of the yellow croaker, *Larimichthys polyactis* (Actinopterygii, Perciformes, Sciaenidae), from the southern Yellow Sea. *Acta Ichthyol. Piscat.* **2021**, *51*, 59–65. [[CrossRef](#)]

25. Nakamura, M.; Yoneda, M.; Ishimura, T.; Shirai, K.; Tamamura, M.; Nishida, K. Temperature dependency equation for chub mackerel (*Scomber japonicus*) identified by a laboratory rearing experiment and microscale analysis. *Mar. Freshw. Res.* **2020**, *71*, 1384–1389. [[CrossRef](#)]
26. Sanchez, P.; Rooker, J.R.; Zapp Sluis, M.; Pinsky, J.; Dance, M.; Falterman, B.; Allman, R. Application of otolith chemistry at multiple life history stages to assess population structure of Warsaw grouper in the Gulf of Mexico. *Mar. Ecol. Prog. Ser.* **2020**, *651*, 111–123. [[CrossRef](#)]
27. Pereira, N.S.; Sial, A.N.; Pinheiro, P.B.; Freitas, F.L.; Silva, A.M.C. Carbon and oxygen stable isotopes of freshwater fish otoliths from the São Francisco River, northeastern Brazil. *An. Acad. Bras. Cienc.* **2021**, *93*, e20191050. [[CrossRef](#)]
28. Shiao, J.C.; Hsu, J.; Cheng, C.C.; Tsai, W.Y.; Lu, H.; Tanaka, Y.; Wang, P. Contribution rates of different spawning and feeding grounds to adult Pacific bluefin tuna (*Thunnus orientalis*) in the northwestern Pacific Ocean. *Deep Sea Res. I* **2021**, *169*, 103453. [[CrossRef](#)]
29. Tripp, A.; Murphy, H.M.; Davoren, G.K. Otolith chemistry reveals natal region of larval capelin in coastal Newfoundland, Canada. *Front. Mar. Sci.* **2020**, *7*, 258. [[CrossRef](#)]
30. Campana, S.E.; Thorrold, S.R. Otoliths, increments, and elements: Keys to a comprehensive understanding of fish populations? *Can. J. Fish. Aquat. Sci.* **2001**, *58*, 30–38. [[CrossRef](#)]
31. Zhang, Z.; Moksness, E. A chemical way of thinning otoliths of adult Atlantic herring (*Clupea harengus*) to expose the microstructure in the nucleus region. *ICES J. Mar. Sci.* **1993**, *50*, 213–217. [[CrossRef](#)]
32. Campana, S.E.; Fowler, A.J. Otolith elemental fingerprinting for stock identification of Atlantic Cod (*Gadus morhua*) using laser ablation ICPMS. *Can. J. Fish. Aquat. Sci.* **1994**, *51*, 1942–1950. [[CrossRef](#)]
33. Itoh, T.; Tsuji, S. Age and growth of juvenile southern bluefin tuna *Thunnus maccoyii* based on otolith microstructure. *Fish. Sci.* **1996**, *62*, 892–896. [[CrossRef](#)]
34. Busbridge, T.A.J.; Marshall, C.T.; Arkhipkin, A.I.; Shcherbich, Z.; Marriott, A.L.; Brickle, P. Can otolith microstructure and elemental fingerprints elucidate the early life history stages of the gadoid southern blue whiting (*Micromesistius australis australis*)? *Fish. Res.* **2020**, *228*, 105572. [[CrossRef](#)]
35. Brickle, P.; Schuchert, P.C.; Arkhipkin, A.I.; Reid, M.R.; Randhawa, H.S. Otolith trace elemental analyses of south American austral hake, *Merluccius australis* (Hutton, 1872) indicates complex salinity structuring on their spawning/larval grounds. *PLoS ONE* **2016**, *11*, e0145479. [[CrossRef](#)]
36. Mu, X.X.; Zhang, C.; Zhang, C.L.; Yang, J.; Ren, Y. Age-structured otolith chemistry profiles revealing the migration of *Conger myriaster* in China Seas. *Fish. Res.* **2021**, *239*, 105938. [[CrossRef](#)]
37. Lee, Y.C.; Chang, P.H.; Shih, C.H.; Shiao, J.C.; Tzeng, T.D.; Chang, W.C. The impact of religious release fish on conservation. *Glob. Ecol. Conser.* **2021**, *27*, e01556. [[CrossRef](#)]
38. Lazartigues, A.; Girard, C.; Brodeur, P.; Lecomte, F.; Mingelbier, M.; Sirois, P. Otolith microchemistry to identify sources of larval yellow perch in a fluvial lake: An approach towards freshwater fish management. *Can. J. Fish. Aquat. Sci.* **2018**, *75*, 474–487. [[CrossRef](#)]
39. Fitzpatrick, R.M.; Winkelman, D.L.; Johnson, B.M. Using isotopic data to evaluate *Esox lucius* (Linnaeus, 1758) natal origins in a hydrologically complex river basin. *Fishes* **2021**, *6*, 67. [[CrossRef](#)]
40. Izzo, C.; Doubleday, Z.A.; Gillanders, B.M. Where do elements bind within the otoliths of fish? *Mar. Freshw. Res.* **2016**, *67*, 1072–1076. [[CrossRef](#)]
41. Thomas, O.R.B.; Ganio, K.; Roberts, B.R.; Swearer, S.E. Trace element-protein interactions in endolymph from the inner ear of fish: Implications for environmental reconstructions using fish otolith chemistry. *Metallomics* **2017**, *9*, 239–249. [[CrossRef](#)] [[PubMed](#)]
42. Hüseyin, K.; Limburg, K.E.; De Pontual, H.; Thomas, O.R.B.; Cook, P.K.; Heimbrand, Y.; Blass, M.; Sturrock, A.M. Trace element patterns in otoliths: The role of biomineralization. *Rev. Fish. Sci. Aquac.* **2020**, *29*, 1–33. [[CrossRef](#)]
43. Jessop, B.M.; Wang, C.H.; Tzeng, W.N.; You, C.F.; Shiao, J.C.; Lin, S.H. Otolith Sr:Ca and Ba:Ca may give inconsistent indications of estuarine habitat use for American eels (*Anguilla rostrata*). *Environ. Biol. Fish.* **2012**, *93*, 193–207. [[CrossRef](#)]
44. Menezes, R.; Moura, P.E.S.; Santos, A.C.A.; Moraes, L.E.; Condini, M.V.; Rosa, R.S.; Albuquerque, C.Q. Habitat use plasticity by the dog snapper (*Lutjanus jocu*) across the Abrolhos Bank shelf, eastern Brazil, inferred from otolith chemistry. *Estuar. Coast. Shelf Sci.* **2021**, *263*, 107637. [[CrossRef](#)]
45. Yuan, C.M.; Qin, A.L.; Liu, R.H.; Lin, J.B. On the classification of the anchovies, *Coilia*, from the lower Yangtze River and the southeast coast of China. *J. Nanjing Univ. (Nat. Sci.)* **1980**, *3*, 67–77, (In Chinese with English Abstract).
46. Khumbanyiwa, D.D.; Li, M.M.; Jiang, T.; Liu, H.B.; Yang, J. Unraveling habitat use of *Coilia nasus* from Qiantang River of China by otolith microchemistry. *Reg. Stud. Mar. Sci.* **2018**, *18*, 122–128. [[CrossRef](#)]
47. Jiang, T.; Liu, H.B.; Shen, X.Q.; Shimasaki, Y.; Ohshima, Y.; Yang, J. Life history variations among different populations of *Coilia nasus* along the Chinese Coast, inferred from otolith microchemistry. *J. Fac. Agric. Kyushu Univ.* **2014**, *59*, 383–389. [[CrossRef](#)]
48. Jiang, T.; Liu, H.B.; Lu, M.J.; Chen, T.T.; Yang, J. A possible connectivity among estuarine tapertail anchovy (*Coilia nasus*) populations in the Yangtze River, Yellow Sea, and Poyang Lake. *Estuar. Coast.* **2016**, *39*, 1762–1768. [[CrossRef](#)]
49. Moura, A.; Dias, E.; López, R.; Antunes, C. Regional population structure of the European eel at the southern limit of its distribution revealed by otolith shape signature. *Fishes* **2022**, *7*, 135. [[CrossRef](#)]
50. Li, Y.; Xie, S.; Li, Z.; Gong, W.; He, W. Gonad development of an anadromous fish *Coilia ectenes* (Engraulidae) in lower reach of Yangtze River, China. *Fish. Sci.* **2007**, *73*, 1224–1230. [[CrossRef](#)]

51. Xu, G.C.; Nie, Z.J.; Zhang, C.X.; Wei, G.L.; Xu, P.; Gu, R.B. Histological studies on testis development of *Coilia nasus* under artificial farming conditions. *J. Huazhong Agric. Univ.* **2012**, *31*, 247–252, (In Chinese with English Abstract). [[CrossRef](#)]
52. Ge, K.K.; Zhong, J.S. Daily-age structure and growth characteristics of *Coilia nasus* larvae and juveniles in the surf zone of Yangtze River Estuary. *Acta Hydro. Sin.* **2010**, *34*, 716–721. [[CrossRef](#)]
53. Dou, S.Z.; Amano, Y.; Yu, X.; Cao, L.; Kotaro, S.; Otake, T.; Tsukamoto, K. Elemental signature in otolith nuclei for stock discrimination of anadromous tapertail anchovy (*Coilia nasus*) using laser ablation ICPMS. *Environ. Biol. Fish.* **2012**, *95*, 431–443. [[CrossRef](#)]
54. Vesanto, J. Neural network tool for data mining: SOM Toolbox. In Proceedings of the 5th International Symposium on Tool Environments and Development Methods for Intelligent Systems (TOOLMET2000), Oulu, Finland, 13–14 April 2000; Oulun Yliopistopaino: Oulu, Finland, 2000; pp. 184–196.
55. Tsai, W.P.; Huang, S.P.; Cheng, S.T.; Shao, K.T.; Chang, F.J. A data-mining framework for exploring the multi-relation between fish species and water quality through self-organizing map. *Sci. Total Environ.* **2017**, *579*, 474–483. [[CrossRef](#)]
56. Wang, C.; Li, X.H.; Lai, Z.N.; Li, Y.F.; Dauta, A.; Lek, S. Patterning and predicting phytoplankton assemblages in a large subtropical river. *Fund. Appl. Limnol.* **2014**, *185*, 263–279. [[CrossRef](#)]
57. Schaffler, J.J.; Young, S.P.; Herrington, S.; Ingram, T.; Tannehill, J. Otolith chemistry to determine within-river origins of Alabama Shad in the Apalachicola-Chattahoochee-Flint River basin. *Trans. Am. Fish. Soc.* **2015**, *144*, 1–10. [[CrossRef](#)]
58. Aschenbrenner, A.; Ferreira, B.P.; Rooker, J.R. Spatial and temporal variability in the otolith chemistry of the Brazilian snapper *Lutjanus alexandrei* from estuarine and coastal environments. *J. Fish Biol.* **2016**, *89*, 753–769. [[CrossRef](#)] [[PubMed](#)]
59. Bouchoucha, M.; Pécheyran, C.; Gonzalez, J.L.; Lenfant, P.; Darnaude, A.M. Otolith fingerprints as natural tags to identify juvenile fish life in ports. *Estuar. Coast. Shelf Sci.* **2018**, *212*, 210–218. [[CrossRef](#)]
60. Jiang, T.; Yang, J.; Liu, H.; Shen, X.Q. Life history of *Coilia nasus* from the Yellow Sea inferred from otolith Sr:Ca ratios. *Environ. Biol. Fish.* **2012**, *95*, 503–508. [[CrossRef](#)]
61. Hane, Y.; Kimura, S.; Yokoyama, Y.; Miyairi, Y.; Ushikubo, T.; Ishimura, T.; Ogawa, N.; Aono, T.; Nishida, K. Reconstruction of temperature experienced by Pacific bluefin tuna *Thunnus orientalis* larvae using SIMS and microvolume CF-IRMS otolith oxygen isotope analyses. *Mar. Ecol. Prog. Ser.* **2020**, *649*, 175–188. [[CrossRef](#)]
62. Yuan, C.M.; Qin, A.L. Ecological habits and distribution of *Coilia* along the Chinese Coast and its changes of output. *Mar. Sci.* **1984**, *5*, 35–37, (In Chinese with English Abstract).
63. Martino, J.C.; Doubleday, Z.A.; Chung, M.T.; Gillanders, B.M. Experimental support towards a metabolic proxy in fish using otolith carbon isotopes. *J. Exp. Biol.* **2020**, *223*, jeb217091. [[CrossRef](#)] [[PubMed](#)]
64. Chung, M.T.; Trueman, C.N.; Godiksen, J.A.; GrønkJær, P. Otolith $\delta^{13}\text{C}$ values as a metabolic proxy: Approaches and mechanical underpinnings. *Mar. Freshw. Res.* **2019**, *70*, 1747. [[CrossRef](#)]
65. Elsdon, T.S.; Ayvazian, S.; McMahon, K.W.; Thorrold, S.R. Experimental evaluation of stable isotope fractionation in fish muscle and otoliths. *Mar. Ecol. Prog. Ser.* **2010**, *408*, 195–205. [[CrossRef](#)]
66. Von Biela, V.R.; Newsome, S.D.; Zimmerman, C.E. Examining the utility of bulk otolith $\delta^{13}\text{C}$ to describe diet in wild-caught black rockfish *Sebastes melanops*. *Aquat. Biol.* **2015**, *23*, 201–208. [[CrossRef](#)]
67. Dittman, A.H.; Quinn, T.P. Homing in Pacific salmon: Mechanisms and ecological basis. *J. Exp. Biol.* **1996**, *199*, 83–91. [[CrossRef](#)]
68. Jiang, T.; Yang, J.; Lu, M.J.; Liu, H.B.; Chen, T.T.; Gao, Y.W. Discovery of a spawning area for anadromous *Coilia nasus* temminck et schlegel, 1846 in Poyang Lake, China. *J. Appl. Ichthyol.* **2017**, *33*, 189–192. [[CrossRef](#)]
69. Brennan, S.R.; Zimmerman, C.E.; Fernandez, D.P.; Cerling, T.E.; Mcphee, M.V.; Wooller, M.J. Strontium isotopes delineate fine-scale natal origins and migration histories of Pacific salmon. *Sci. Adv.* **2015**, *1*, e1400124. [[CrossRef](#)]
70. Yano, K.; Nakamura, A. Observations on the effect of visual and olfactory ablation on the swimming behavior of migrating adult chum salmon, *Oncorhynchus keta*. *Jpn. J. Ichthyol.* **1992**, *39*, 67–83. [[CrossRef](#)]
71. Zhu, G.; Wang, L.; Tang, W.; Wang, X.; Wang, C. Identification of olfactory receptor genes in the Japanese grenadier anchovy *Coilia nasus*. *Genes Genom.* **2017**, *39*, 521–532. [[CrossRef](#)]